Construction and Building Materials 220 (2019) 64–75

Contents lists available at ScienceDirect

Construction and Building Materials

journal homepage: www.elsevier.com/locate/conbuildmat

The effects of hollow glass microsphere modification on the road performances and thermal performance of asphalt binder and mixture

Chao Feng [a], Hongliang Zhang [a,*], Changjin li [a], Wei Jia [a,b], Feng Lai [a,c]

[a] Key Laboratory for Special Area Highway Engineering of Ministry of Education, Chang'an University, Xi'an, Shaanxi 710064, PR China
[b] Guangdong Provincial Communication Planning and Design Institute Co., Ltd, Guangzhou City 510000, PR China
[c] Guangdong Nanyue Transportation Investment Construction Co., Ltd, Guangzhou City 510000, PR China

HIGHLIGHTS

- HGM and HGM/SBS modified asphalts and their mixtures are prepared.
- HGM increases high temperature stability and decreases low temperature performance of asphalts.
- HGM improves the cooling, high-temperature and low-temperature performances of AC-13.
- HGM has no obvious effect on cooling performance of SMA-13 mixture.
- It is recommended to use 5% HGM modified AC-13 mixture.

ARTICLE INFO

Article history:
Received 15 November 2018
Received in revised form 25 April 2019
Accepted 29 May 2019
Available online 6 June 2019

Keywords:
Thermal resistance pavement
Hollow glass microsphere
Modified asphalt
Asphalt mixture
Cooling performance
Road performance

ABSTRACT

High temperature in asphalt pavements often leads to rutting of asphalt pavements and heat island effects in urban areas. In this study, to improve the thermal resistance of asphalt pavement, hollow glass microspheres (HGM) modified asphalt and HGM/Styrene-Butadiene-Styrene (SBS) modified asphalt were used to prepare asphalt concrete (AC) and stone mastic asphalt (SMA) respectively. The effects of HGM on the penetration, ductility, softening point and rheological properties of asphalt binder and the cooling performance, mechanical property, high temperature stability, low temperature resistance, water stability and other properties of asphalt mixture were investigated. Finally, the composition of the thermal resistance surface layer was recommended. Results showed that, adding HGM increased the high temperature stability of both matrix asphalt and SBS modified asphalt while the low temperature performance of both the two types of asphalts decreased. For the asphalt mixture, the addition of HGM improved the cooling performance of the AC-13 mixture but had no effect on the cooling performance of the SMA-13 mixture. HGM also showed positive effects on the pavement performance of the asphalt mixtures. For the AC-13 mixture, it improved the mechanical property, high-temperature stability, low-temperature cracking resistance and immersion residue stability but had no effect on the thaw-splitting strength ratio (*TSR*). For the SMA-13 mixture, it improved the Marshall stability, high-temperature stability, immersion residue stability, scattering resistance while impaired the low-temperature crack resistance, *TSR* and anti-drainage ability. Finally, it was recommended to use 5% HGM modified AC-13 mixture as the thermal resistance surface layer.

1. Introduction

Due to its dark color, asphalt mixture has a high solar radiation absorption rate in the natural environment. Long sunshine exposure causes the asphalt pavement to absorb a large amount of heat, resulting in the continuous increase of the road surface temperature and rutting. As one of the most typical and extensive forms of distress, rutting reduces the comfort and safety of driving, affects the performance of asphalt pavement [1]. Besides, the high temperature of road surface also causes urban heat island effect in cities [2]. The heat accumulated due to heat island effect also leads to urban heating, aggravates air pollution and causes harm to residents' health [3]. In order to reduce the negative impact of high temperature on the road surface, many measures have been taken. Among which, cooling asphalt pavement is considered as a viable

* Corresponding author.
E-mail address: zhliang0105@163.com (H. Zhang).

https://doi.org/10.1016/j.conbuildmat.2019.05.183
0950-0618/

approach [4,5]. In the past years, the techniques of solar reflective coating [6], retro reflective films [7], thermochromic coating [8,9], phase-change material [10–12], solar collector pavement [13,14] and thermal resistance pavement [15–24] have been applied to develop cooling asphalt pavement. Among these techniques, thermal resistance pavement is one of the most effective techniques.

Thermal resistance pavement is one kind of pavements with an insulation effect and can impede heat from transferring inside the asphalt pavement, thereby reducing the internal temperature of the pavement. The cooling effect is usually achieved by increasing the void ratio in pavement or adding a material with a lower thermal conductivity into the asphalt mixture to change the temperature conductivity of the asphalt mixture. Porous pavement, water retaining pavement and thermal resistance aggregate pavement are three most common types of thermal resistance pavements.

In terms of porous pavement, Cahill et al. [15] found that the application of macroporous mixture could reduce thermal conductivity by 30%–60%. Liu et al. [16] added a capillary column to the conventional porous pavement structure to develop a new type of permeable pavement called evaporation-enhancing permeable pavement. The capillary column could increase the evaporation of the road surface, thereby reducing the temperature of pavement surface. Chen et al. [17] investigated the performances of Porous Polyurethane Mixture (PPM), and found that PPM can reduce the temperature inside the pavement by 1 °C–3 °C.

For water retaining pavement, Higashiyama et al. [18] poured several cement-based grouting materials into voids of porous asphalt pavements to investigate the temperature of surface. The results showed that this water retaining pavement could reduce the surface temperature significantly. Wang et al. [19] employed partial immersion tests and evaporative cooling tests on open-graded permeable concrete (PC) and sintered ceramic porous brick (CB). It was found that the water absorption rate of CB was higher than that of PC.

As far as thermal resistance aggregate pavement is concerned, Benrazavi et al. [20] tested four different pavement materials of Fontana concrete (FC), Rosa Tanggo polished granite (RTPG), Blue Impala polished granite (BIPG) and asphalt (AS) in three different environments namely open space, under shade and near water to investigate their surface temperatures. The results indicated that, in open space locations, BIPG was 15.5 °C cooler than AS during 12:00 to 15:00. However, during 12:00 to 18:00, the temperatures of BIPG and RTPG specimens' surface increased in near water locations compared to open space and under shaded locations. Chen et al. [21] investigated the effect of adding recycled tire rubber (RTR) powder on the thermal performance of asphalt and asphalt mixture. The experimental results showed that, when the filler was replaced by 100% crumb rubber, the thermal conductivity of the asphalt mixture decreased by 19.8%. But the addition of RTR also decreased the heat capacity of asphalt mortar and the moisture resistance of asphalt mixture. Liu et al. [22] found that by replacing the coarse aggregate with calcined bauxite could reduce the temperature of pavement surface by 3.5 °C. However, calcined bauxite was only suitable for pavement in arid areas because the poor water stability of the mixture. Yang [23] replaced the fine aggregate with an equal proportion of vermiculite to prepare asphalt concrete (AC) and a stone mastic asphalt (SMA) with the maximum nominal size of aggregate of 13 mm. The pavement performance test results showed that the incorporation of vermiculite had different degrees of damage to the water stabilities of the SMA mixture and the AC mixture. It was concluded that the AC mixture with vermiculite could not be used on asphalt pavement while the SMA mixture could. For SMA, when the amount of vermiculite in SMA mixture is 50% by the weight of fine aggregate, the cooling effect is about 3.5 °C. Zhao [24] replaced aggregates with ceramic particles in asphalt mixture. The test results showed that when the common aggregates were all replaced by ceramics, the cooling effect could reach 6 °C. The replacement with ceramics, however, reduced the high temperature stability and water stability of the asphalt mixture. Finally, it was determined that the optimum replacement amount of ceramic in the asphalt mixture was about 40%, and in this case the temperature drop was about 3.7 °C.

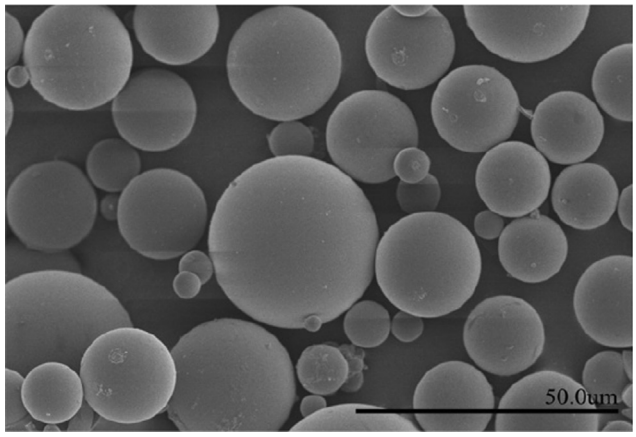

Fig. 1. SEM image of hollow glass microspheres [33].

The hollow glass microsphere (HGM), is a powdery hollow white ball extracted from industrial waste ash. The SEM image of hollow glass microspheres is shown in Fig. 1. It has a particle size of 10–200 μm, a compressive strength of 120 MPa, and exhibits low thermal conductivity, excellent mobility and low density [25–27]. In addition, HGM has been used in plastics industry, coating systems and rubber industry [28–31] due to its high mechanical performance and low production cost. Furthermore, excellent thermal insulation properties make HGM widely used as thermal insulation materials in the building industry [30]. In this study, it was hypothesized that incorporating HGM into asphalt pavement may reduce the temperature of the road surface. However, the related research has not been reported in the literature.

This study aims to investigate the effect on cooling performance and pavement performance of HGM incorporated asphalt mixture. First, Styrene-Butadiene-Styrene (SBS) modified asphalt and HGM/SBS modified asphalt binders were prepared. The effects of HGM on the consistency properties, high and low temperature properties of asphalt binders were studied. Then HGM and HGM/ SBS modified asphalt mixtures were manufactured and the effects of HGM on the cooling effect and road performances of asphalt mixtures were evaluated. According to the test results, finally, the composition of the thermal resistance surface layer was recommended.

2. Materials and methods

2.1. Materials

2.1.1. Hollow glass microspheres (HGM)

The HGM is a white hollow sphere in micron scale, and its properties provided by Shanghai Zhenxu Chemical Co., Ltd are shown in Table 1.

2.1.2. Matrix asphalt and SBS modified asphalt

The future test road will be built in Xi'an, Shaanxi Province. According to the local climate, PG 58-16 asphalt is often used in highway construction. For freeways with a large cumulative traffic axle load, 4% SBS is often added for modification. Therefore, PG 58-16 asphalt and 4% SBS modified asphalt were selected as test asphalts. The properties of two types of asphalt provided by Shell are shown in Tables 2 and 3 respectively.

Table 1
Properties of HGM.

Particle size (μm)	Density (g/cm^3)	Water-soluble	Compressive strength (MPa)	Softening temperature(°C)	Thermal Conductivity (W/m·°C)
15–50	0.425	Insoluble	40–60	600	0.028–0.03

Table 2
Properties of matrix asphalt.

Test item		Results	Acceptance limits in China [34]
Penetration (25 °C, 100 g, 5 s)(0.1 mm)		84.3	80–100
Softening point (R&B method)(°C)		46.5	≥45
Ductility (5 cm/min, 10 °C)(cm)		> 100	≥20
Dynamic viscosity (60 °C)(Pa·S)		158.7	≤160
Thin film oven test (TFOT)	Mass loss (%)	0.051	−0.8–+0.8
	Penetration ratio (%)	67.3	≥57
	Ductility (5 cm/min,10 °C)(cm)	12	≥8
Relative density(25 °C)		1.012	–

Table 3
Properties of SBS modified asphalt.

Test item		Results	Acceptance limits in China [35]
Penetration (25 °C, 100 g, 5 s)(0.1 mm)		55.7	30–60
Softening point (R&B method)(°C)		80.9	≥60
Ductility (5 cm/min, 10 °C)(cm)		37.4	≥20
Dynamic viscosity (60 °C)(Pa·S)		2.19	≤3
Thin film oven test (TFOT)	Mass loss (%)	−0.041	−1–+1
	Penetration ratio (%)	70.3	≥60
	Ductility (5 cm/min, 10 °C)(cm)	24	≥20
Relative density (25 °C)		1.030	–

2.1.3. Preparation of HGM modified asphalt

HGM was used to modify matrix asphalt and SBS modified asphalt. The modification was achieved by the combination of mechanical stirring and high-speed shearing. First, the surface of the HGM was organically activated with silane coupling agent. According to the standard JTG F40-2004 [33], the temperatures ranged from 160 °C to 170 °C for matrix asphalt and from 170 °C to 180 °C for SBS modified asphalt were selected as test temperatures. Based on trial and error, 2000 r/min was selected from the stirring speeds of 1000 r/min, 1500 r/min, 2000 r/min, 2500 r/min, 3000 r/min. During stirring period, the activated HGM was slowly added. Then, the asphalt was sheared for 40 min at the speed of 3000 r/min while kept the temperature constant until the HGM and asphalt were fully mixed.

2.1.4. Asphalt mixture design

The HGM modified asphalt and HGM/SBS modified asphalt prepared in the previous section "Preparation of HGM modified asphalt" were used to prepare the AC mixture and the SMA mixture with the same maximum aggregate particle size of 13 mm respectively. They were noted as AC-13 and SMA-13 respectively. The Basalt was selected as aggregate. The aggregate gradations in these two asphalt mixtures are shown in Fig. 2. According to Marshall test in ASTM D6927 [34], the optimum asphalt aggregate ratios for the AC-13 and SMA-13 mixtures were determined as 5.0% and 6.2%, respectively.

2.2. Test methods

Because of the goal of this study is to investigate the cooling performance of HGM on AC-13 and SMA-13 mixtures, a non-standard cooling test was designed and used. At the meantime, the incorporation of HGM into the asphalt may affect the conventional performance of asphalt binder or asphalt mixture, and may even have adverse effects. Therefore, the influences of the HGM on the conventional performance of asphalt binder and mixture were also evaluated by standard testing methods.

In the conventional performance test of asphalt, penetration, softening point and ductility tests were first carried out to measure the effects of HGM on the viscosity, high temperature performance and low temperature tensile property of the matrix asphalt and the SBS modified asphalt respectively. Then, the dynamic shear rheology (DSR) test and the bending beam rheology (BBR) test were carried out to evaluate the high temperature rheological properties and low temperature crack resistance of the HGM modified asphalt and the HGM/SBS modified asphalt.

The choice of asphalt mixture test depended on the performance requirements of the asphalt pavement. First, the basic Marshall test was carried out. The Marshall stability and flow value obtained from the test were used to evaluate the mechanical properties of AC-13 mixture and SMA-13 mixture. Then, the effects of HGM on the high temperature stability and low temperature crack resistance of the two mixtures were analyzed by Chinese wheel tracking test and low temperature bending beam test respectively. Immersed Marshall test and Freeze-thaw split test were used to analyze the water stability of the two mixtures. Finally, because the large asphalt content and surface depth of the SMA-13 mixture, the Schellenberg binder drainage test and the Cantabro test were performed on the SMA-13 mixture alone to test the effect of HGM on the drainage ability and anti-scattering ability. Refer to Fig. 3 for the specific tests.

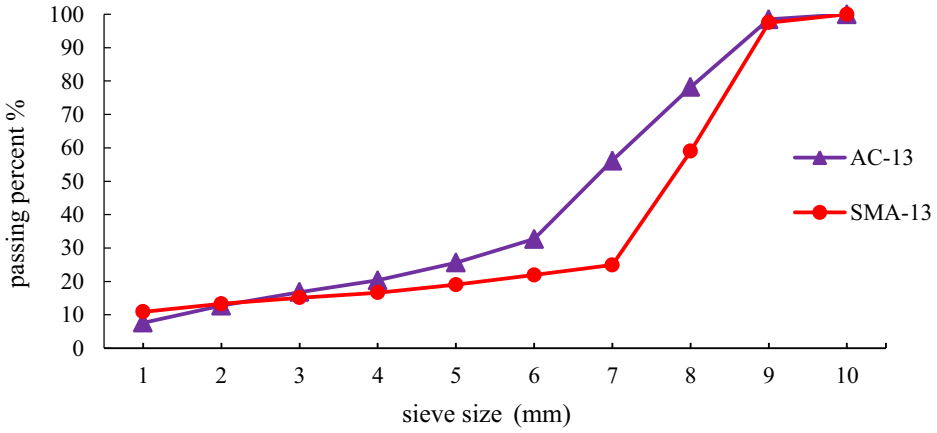

Fig. 2. Gradation curve of AC-13 and SMA-13.

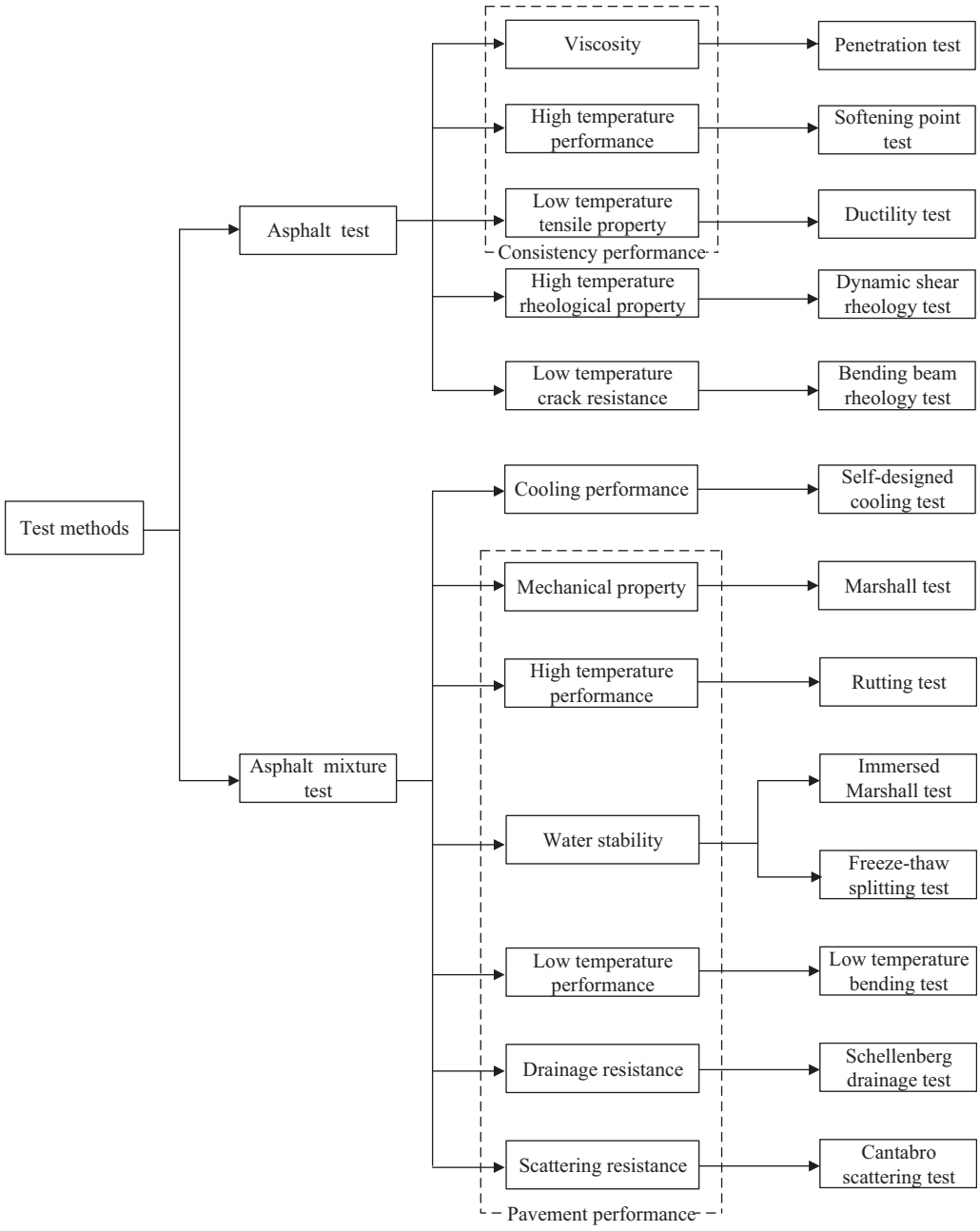

Fig. 3. Test methods.

2.2.1. Performance tests of asphalt binder

2.2.1.1. Consistency tests. In accordance with ASTM D5 [37], the penetration test was conducted. Three vessels containing the asphalt sample were placed in a water bath at 25 °C and were subjected to an applied load of 100 g. Then, the penetration depth (0.1 mm) of the needle in 5 s was measured. The final result was averaged and the allowable error of the test was 0.2 mm.

The softening point test was carried out in accordance with ASTM D36 [38], which employed Ring Ball method. The copper ring containing the asphalt sample was placed in a water bath with an inner diameter of 18.9 mm. Then, a steel ball with a weight of 3.5 g was placed on the sample and the sample was heated with a rate of 5 °C/min to test the temperature at which the pitch softened to a prescribed distance. The same test was taken for three times and the results were averaged. In addition, the allowable error was 2 °C.

According to ASTM D113 [39], the ductility test was conducted. The test pieces were subjected to a tensile rate of 5 cm/min in the test temperature of 10 °C. There were three trials for each test. When the difference between a test value and the average is greater than 20%, the data was discarded.

2.2.1.2. Dynamic shear rheology (DSR) test. According to the requirements of ASTM D7175-15 [40], cylindrical test pieces had a diameter of 25 mm and a height of 1 mm and were loaded at 10 rad/s. Since the later test road will also be carried out in Xi'an, Shaanxi Province, so the maximum temperature of the local summer pavement was taken into account when selecting the test temperature. The highest summer temperature of pavement in Xi'an is 70 °C, therefore, this temperature was selected as the median value, and 58 °C, 64 °C, 70 °C, 76 °C, and 82 °C were selected as the test temperatures for the DSR test of HGM modified asphalt. However, the addition of SBS significantly improved the high temperature performance of asphalt, as a result the shear deformation of HGM/SBS modified asphalt was too small under the temperature below 70 °C. Therefore, for HGM/SBS modified asphalt, only the test temperature not lower than 70 °C were adopted. Two indicators that can be used to characterize the high temperature rheological properties of asphalt binders are the complex modulus (G^*) and phase angle (δ), which can be obtained through experimentation. G^* is an indicator that characterizes the stiffness or deformation resistance of asphalt binders under load. With an increase of G^* value, the resistance to deformation by the asphalt binder increases. δ is a relative indicator of the recoverable and non-recoverable deformation, which ranges from 90° to 0°. The smaller the δ value is, the greater the elasticity, the better high temperature performance and the stronger rutting resistance the asphalt binder will be. In addition, the rutting parameter $G^*/\sin\delta$ can also be used to characterize the high temperature rheological properties of the asphalt binder. With the increase of $G^*/\sin\delta$, the rheology and the stiffer of asphalt binder decreases. Three trials were performed in parallel for each test. The test error of $G^*/\sin\delta$ could not exceed 6.4% of average value.

2.2.1.3. Bending beam rheology (BBR) test. In accordance with the standard of ASTM D6648-08 [41], a 127 mm long, 6.35 mm wide, and 12.7 mm high bituminous beam was used and placed in a liquid bath at −18 °C. The creep stiffness modulus (S) and creep curve slope (m) were collected every 60 s. The indicator S characterizes the ability of asphalt to resist load. The smaller the S value, the better the low temperature flexibility of the asphalt is. The slope of the m value reflects the sensitivity of the asphalt stiffness over time and the stress relaxation ability. The larger the value of m, the better the stress relaxation ability and the better crack resistance of the asphalt is. There were three trials performed during each test, and the result were averaged. For creep stiffness modulus (S) and creep curve slope (m), the respective allowable error were 7.2% and 2.9% of the average.

2.2.2. Cooling test of asphalt mixtures

Considering that test results in outdoor field were susceptible to illumination, rainfall, wind speed and other uncontrolled factors, the cooling effect or the thermal insulation performance of materials could not be accurately evaluated. Therefore, an indoor simulated solar radiation test system shown in Fig. 3 was designed which was consisted of thermal radiation source, incubator, temperature sensor, a data recorder and Recorder 2000 data processing software.

As Fig. 4 shows, the temperature-testing system mainly consists of three parts: iodine-tungsten lamp, tempered glass box and insulation foam board. The first is the iodine-tungsten lamp, which is used to simulate solar radiation and is suspended at a distance of 40 cm from the bottom. The size of the glass box is 450 × 450 × 250 mm and the thickness is 6 mm. An insulating foam board placed on the bottom of the box is used for fixing the AC-13 and SMA-13 test pieces. After 7 h of irradiation, the temperature on the surface of the specimen was kept stable at 60 °C. During the test, the temperatures of the upper surface and lower surface of the specimen were recorded every 30 min by a data logger with an accuracy of 0.1 °C.

2.2.3. Pavement performance tests

2.2.3.1. Marshall test. According to the ASTM D6927 [36], a cylindrical specimen with a diameter of 101.6 mm and a height of 63.5 mm was loaded at a loading rate of 50 mm/min under 60 °C. The Marshall stability and flow value were used respectively to characterize the maximum load carried by the specimen before failure and the amount of the deformation of the specimen. There were four trials for each test. When the difference between a test value and the average was greater than 1.46 times of the standard deviation, the test value was discarded. The average of the remaining values would be used as the test result.

2.2.3.2. Chinese wheel tracking test. By the reciprocating relative movement of the specimen and the wheel at a specified temperature, the specimens were compacted, sheared, pushed and flowed to generate a rut under the repeated action of the wheel. The deformation and test time of the specimen were recorded According to T 0719-2011 of JTG E20-2011 [34], three specimens (300 mm in length, 300 mm in width and 50 mm in height) were prepared. Then a load of 0.7 MPa was applied to the specimens at 60 °C. The evaluation index is dynamic stability (*DS*), which refers to

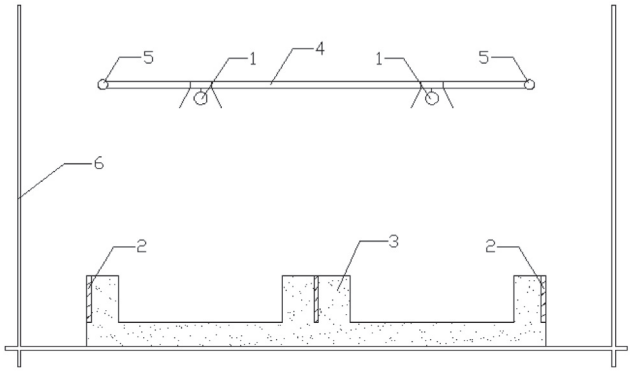

1. Iodine-tungsten lamp; 2. Plywood; 3. Insulation foam board; 4. Lateral bracket; 5. Front and rear bracket; 6. Tempered glass box

Fig. 4. Schematic diagram of temperature test system.

the number of revolutions of the wheel corresponding to 1 mm deformation of the asphalt mixture under high temperature conditions. The higher the *DS*, the better the high temperature stability of the mixture. The coefficient of variation of the dynamic stability in a test could not exceed 20%, and the average value was taken as the result.

2.2.3.3. Immersed Marshall test. In accordance of ASTM D6927 [36] standard, a cylindrical specimen (101.6 mm in diameter and 63.5 mm in height) was prepared and placed in a thermostatic bath at 60 °C for 48 h. And then, a load of 50 mm/min was applied on the specimen. Through the test, the Marshall stability of the specimens after being immersed in the water bath of 60 °C for 48 h and the Marshall stability of the specimens after being soaked for 0.5 h at the same temperature were obtained. Finally, the immersion residual stability was calculated using Eq. (1). The greater the immersion residual stability, the better the water stability of the mixture is. Four replicates were for each test. The allowable error is the same as the Marshall test.

$$MS_0 = \frac{MS_1}{MS} \times 100\% \quad (1)$$

where MS_0 is the immersion residual stability (%), MS_1 is the stability after bathing for 48 h, and *MS* is the residual stability after bathing for 0.5 h.

2.2.3.4. Freeze-thaw splitting test. Freeze-thaw splitting test was used to evaluate the water stability of asphalt mixture by measuring the splitting strength ratio of the asphalt mixtures before and after the freeze-thaw cycle under the specified conditions. The larger the ratio, the better the water stability of the asphalt mixture. In the light of the standard AASHTO T 283 [42], eight cylindrical specimens (101.6 mm in diameter and 63.5 mm in height) were prepared and were divided into two groups. The first group were kept at room temperature. The second group first were vacuum-saturated under a vacuum of 80.0 KPa and then were placed in a thermostatic bath at 60 °C for 24 h. Next, the second group of specimens were placed in a low temperature −18 °C environment for 16 h. Finally, the two groups of test pieces were placed in a thermostatic bath at 25 °C for 2 h and then were taken out. The splitting test was performed at a loading rate of 50 mm/min. The ratio of freeze-thaw splitting strength was calculated by Eq. (2).

$$TSR = \frac{\delta_2}{\delta_1} \times 100\% \quad (2)$$

where *TSR*, δ_1 and δ_2 are the ratio of freeze-thaw splitting strength (%), the splitting strength (MPa) under standard conditions, and the splitting strength (MPa) after a freeze-thaw cycle under specified conditions, respectively. For the two splitting strengths, the value was discarded when the difference between the value and the average was greater than 1.46 times of the standard deviation, the average of the remaining values were used as the result.

2.2.3.5. Low-temperature bending test. According to the method T 0715 of JTG E20-2011 [34], a prismatic beam (250 mm in length, 30 mm in width, and 35 mm in height) was prepared. After 45 min of soaking at −10 °C, a load of 50 mm/min was applied. The bending deflection of the beam during the experiment was recorded by the sensor, and the maximum bending strain at the bottom of the beam was calculated by the Eq. (3).

$$\varepsilon_B = 6hd/L^2 \quad (3)$$

where ε_B was the maximum bending strain at the bottom of the beam (με), *h* was the height of mid-span cross-section of specimen (mm), and *d* was the deflection of mid-span of specimen (mm), *L* was the span of specimen (mm).

The maximum bending strain is an important index for evaluating the low-temperature crack resistance of asphalt mixture, an increase in the index value, and results in an increase in the low-temperature crack resistance of the mixture. For each asphalt mixture, three replicates were prepared during the test. The differences between the value and the average could not be greater than 1.15 times of the standard deviation.

2.2.3.6. Schellenberg binder drainage test. According to the method T 032 of JTG E20-2011 [32], 1 kg of asphalt mixture was added into an 800 ml dry beaker, and then the beaker was placed in an oven at 185 °C for 60 min. Finally, the mass loss during this period was measured. Three replicates were for each test, and the final data were the average value of every experiment. In the measurement process, the allowable error of the test piece weight was 0.1 g.

2.2.3.7. Cantabro test. The test was performed in accordance with T 0733 of JTG E20-2011 [32]. A cylindrical Marshall specimen (101.6 mm in diameter, 63.5 mm in height) was prepared. The test pieces were placed in a thermostatic bath at 20 °C for 20 h and then wiped and weighed. The test piece was then placed in a Los Angeles testing machine to rotate 300 rpm at 30r/min and then was weighed again. Finally the mass loss of the mixture in the Cantabro test was calculated. Three replicates were for each test and the final data were the average value of every experiment. The allowable error of the test was 0.1 g.

3. Results and discussions

3.1. Properties of asphalt binder

3.1.1. Consistency properties

Penetration, ductility and softening point tests were conducted for HGM modified asphalt with HGM of 3%, 4%, 5% and 6% by the weight of matrix asphalt, HGM/SBS modified asphalt with 4% SBS and HGM of 3%, 4%, 5% and 6% by the weight of matrix asphalt. The results are shown in Table 4. It can be seen that, for both the matrix asphalt and SBS modified asphalt, the addition of the HGM impaired the penetration. With the increase in the content of HGM, the penetration decreased.

In terms of the effects on softening point, for the matrix asphalt, the softening point increased after the HGM was incorporated with the increase of the amount of HGM to a small extent. But for the SBS modified asphalt, when the content of the HGM increased from 0% to 6%, the softening point first increased and then decreased. When the amount of HGM was 4%, the softening point reached the peak 98.6 °C.

Regarding the effects on ductility, the addition of HGM led to a significant decrease in the ductility of asphalt. When the HGM dosage was 6% for matrix asphalt and 5% or 6% for SBS modified asphalt, the ductility cannot meet the specification requirements of greater than 20 cm in China. Therefore, HGM modified asphalt with HGM of 3, 4 and 5%, HGM/SBS modified asphalt with HGM of 3 and 4% were selected to be subjected to DSR and BBR tests.

The above phenomenon may be caused by the addition of HGM which changes the composition of the asphalt. When the amount of HGM increases from 3% to 4%, the non-bonding between HGM and asphalt molecules makes part of HGM into the center of micelles, increases the content of asphaltene and reduces the content of light components [43]. When the amount of HGM increases from 5% to 6%, part of the excessive HGM acts as a filler in the asphalt, which hinders the movement of the asphalt molecules thereby reducing penetration. When the amount of HGM increases from 4% to 5%, HGM not only produces non-bonding with the

Table 4
Consistency properties of asphalt.

Asphalt	Consistency indexes		
	Penetration (25 °C, 100 g,5s)(0.1 mm)	Softening point (°C)	Ductility (5 cm/min, 10 °C) (cm)
Matrix asphalt	84.3	46.5	>100
3%HGM modified asphalt	69.6	47.5	27.8
4%HGM modified asphalt	67.5	47.7	26.7
5%HGM modified asphalt	62.3	47.8	23.5
6%HGM modified asphalt	60.5	48.4	19.2
4%SBS modified asphalt	55.7	80.9	37.4
3%HGM + 4%SBS modified asphalt	49.3	88.4	29.2
4%HGM + 4%SBS modified asphalt	46.4	>90	27.3
5%HGM + 4%SBS modified asphalt	44.7	87.5	16.8
6%HGM + 4%SBS modified asphalt	42.5	61.8	14.0

asphalt molecules, but also plays the filling effect, so the penetration improvement caused by this part was significant. Therefore, the increase in viscosity and high temperature properties of the asphalt caused by the addition of HGM results in an increase in the penetration and softening point of the matrix asphalt and the SBS modified asphalt. In addition, HGM is an inorganic rigid particle. Under the action of tension, HGM does not produce elongation deformation, which causes debonding of the joint surface between asphalt and HGM [44]. As a result, stress concentration occurs at the interface and the ductility of the asphalt decreased.

3.1.2. High temperature performance

The DSR test was carried out in accordance with the regulations of ASTM D7175 [40] and the test results are shown in Tables 5 and 6.

According to Tables 5 and 6, it can be seen that, at the same temperature and for both of matrix asphalt and SBS modified asphalt, the incorporation of HGM increased the rutting factor, and as the HGM content increased the rutting factor increased. For example, at 58 °C, the rutting factors of 3%, 4%, and 5% HGM modified asphalt increased by 43.8%, 44.7% and 138.5% respectively compared with that of the matrix asphalt. Compared to the rutting factor of 4% SBS modified asphalt, the rutting factors of 3% HGM + 4% SBS modified asphalt and 4% HGM + 4% SBS modified asphalt increased by 18.2% and 26.3% at 70 °C respectively. The main reason for the improvement of the rutting factor of modified asphalt may be similar to that for the improvement of softening point. The addition of HGM increases the viscosity of asphalt and improves the high temperature shear resistance of asphalt effectively.

3.1.3. Low temperature performance

BBR was used to evaluate the rheological properties of asphalt binder at low temperature. The selected test temperature was −18 °C, and the measured creep modulus S and creep curve slope m of different asphalts are shown in Figs. 5 and 6.

Table 5
DSR test results of matrix asphalt and HGM modified asphalt.

Test item	Temperature (°C)	Asphalt			
		Matrix asphalt	3%HGM modified asphalt	4%HGM Modified asphalt	5%HGM modified asphalt
Complex shear modulus G^*(kPa)	58	2.221	3.199	3.219	5.218
	64	1.058	1.370	1.387	2.638
	70	0.5503	0.6446	0.6525	1.366
	76	0.2611	0.3282	0.3341	0.6546
	82	0.1476	0.1813	0.1842	0.3251
Phase angle δ(°)	58	85.30	86.96	87.01	79.04
	64	86.17	87.69	87.87	80.29
	70	87.20	88.51	88.75	80.89
	76	87.89	88.79	88.96	81.44
	82	88.23	89.11	89.41	82.11
Rutting factor $G^*/sin\delta$(kPa)	58	2.228	3.204	3.224	5.315
	64	1.060	1.371	1.388	2.676
	70	0.5510	0.6448	0.6527	1.383
	76	0.2613	0.3281	0.3342	0.6620
	82	0.1475	0.1812	0.1842	0.3282

Table 6
DSR test results of SBS and HGM/SBS modified asphalt.

Test item	Temperature (°C)	Asphalt		
		4%SBS modified asphalt	3%HGM + 4%SBS modified asphalt	4%HGM + 4%SBS modified asphalt
Complex shear modulus G^*(kPa)	70	1.852	2.245	2.311
	76	1.066	1.243	1.279
	82	0.6714	0.7492	0.8255
Phase angle δ(°)	70	70.94	75.69	68.97
	76	71.68	76.24	69.51
	82	72.55	77.96	70.11
Rutting factor $G^*/sin\delta$(kPa)	70	1.960	2.317	2.476
	76	1.123	1.280	1.365
	82	0.7037	0.7661	0.8747

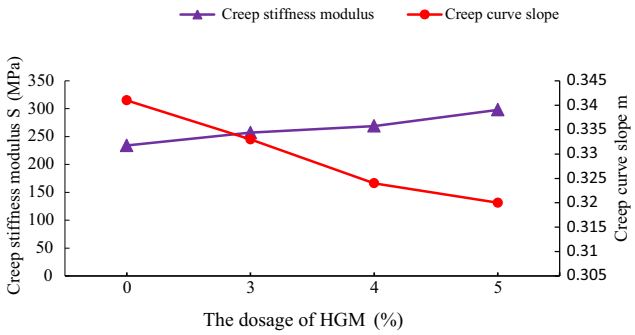

Fig. 5. BBR test results of matrix asphalt and HGM modified asphalt.

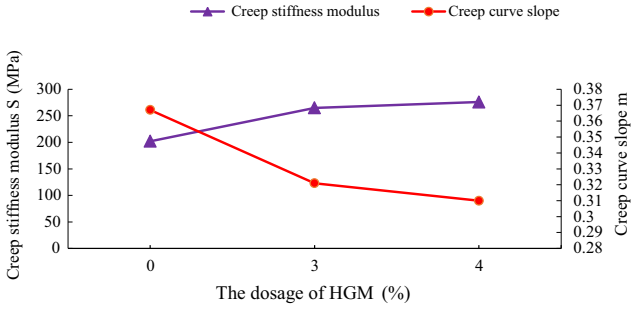

Fig. 6. BBR test results of SBS and HGM/SBS modified asphalt.

At the low temperature of −18 °C, with the increase in the dosage of HGM, the creep modulus *S* of HGM modified asphalt and HGM/SBS modified asphalt obviously increased. For matrix asphalt, the addition of 3%, 4% and 5% HGM increased the creep modulus *S* of the asphalt by 9.8%, 14.9% and 27.3%, respectively. Similarly, the addition of 3% and 4% HGM into 4%SBS modified asphalt increased the creep modulus of the SBS modified asphalt by 31.1% and 36.6% respectively. On the contrary, the addition of HGM decreased the creep curve slope *m* for both matrix asphalt and SBS modified asphalt. The greater HGM content resulted in lower creep curve value. According to the effects on the creep modulus *S* and the creep curve slope *m*, it can be concluded that the addition of HGM can reduce the low temperature crack resistance of both matrix and SBS modified asphalts. This phenomenon can be explained by the decrease in ductility. The incorporation of HGM reduced the ductility of asphalt under low temperature conditions, which can reflect the low temperature crack resistance of asphalt.

3.2. Cooling effect of HGM modified asphalt mixture

A temperature test system was designed and used to measure the temperatures at the top and bottom of different types of asphalt mixture samples. The cooling effect can be obtained by subtracting the temperature difference of the asphalt mixture with different amounts of HGM from the temperature difference of the asphalt mixture without HGM at the same time. The cooling effects of the AC-13 mixture and the SMA-13 mixture with different amounts of HGM are discussed below.

3.2.1. Cooling effect of AC-13 mixture

The histories of the temperatures at the top and bottom of specimen and their differences are listed in Table 7. On the one hand, as the heating time increased, the temperature differences of the mixture specimens first increased and then decreased. When the heating time was 1 h, the temperature differences of all of the specimens reach the peak. On the other hand, when HGM was added, the temperature differences between the top and bottom of specimens become larger. With the increase in HGM content, the cooling effect increased. For example, when the content of HGM was 3%, 4% and 5% the maximum temperature difference improvements are 1.2 °C, 2.4 °C and 2.9 °C respectively.

The cooling mechanism of HGM may be related to the principle of heat transfer. The heat flow paths of asphalt mixture can be divided into two types: one is through the gap and the continuous asphalt binder, and the other is through the aggregate and the discontinuous asphalt binder. By adding HGM to increase the micro void of the asphalt binder, the thermal conductivity of the asphalt binder can be reduced. As a result, the thermal conductivity of the AC-13 mixture reduced.

3.2.2. Cooling effect of SMA-13 mixture

The SMA-13 specimens with 0%, 3% and 4% HGM were selected to be subjected to the same temperature test as AC-13 mixture, and the results are shown in Table 8. It can be seen that, as the heating time increased, the temperature differences of the SMA mixtures first increased and then decreased and peak at the time of 1 h. However, compared with the SMA-13 specimens without HGM, the cooling effect caused by the addition of HGM was not obvious. During the test period, the maximum cooling effects of 3% and 4% HGM were 0.7 °C and 0.5 °C, respectively. It may be due to the large amount of asphalt used in SMA-13 mixture, the small thermal conductivity of the asphalt itself, and the relatively small amount of HGM.

Table 7
Temperature test results of AC-13 mixture.

HGM Dosage (%)	Index	Measured temperature (°C) at different time (h)														
		0.0	0.5	1.0	1.5	2.0	2.5	3.0	3.5	4.0	4.5	5.0	5.5	6.0	6.5	7.0
0	Top	10.1	24.5	36.7	40.9	44.3	47.1	49.7	51.3	52.9	54.5	55.4	56.5	57.6	59	60.2
	Bottom	10.1	13.3	19.4	24.8	28.9	34.2	38.3	42.4	46.9	51	53.4	55.7	57	58.6	59.9
	Difference	0.0	11.2	17.3	16.1	15.4	12.9	11.4	8.9	6.0	3.5	2.0	0.8	0.6	0.4	0.3
3	Top	10.3	25.2	37.1	41.3	44.6	47.7	50	51.5	53.2	54.5	55.5	56.4	57.6	58.9	60.1
	Bottom	10.3	13.9	19.6	24.8	28.5	33.8	37.6	41.5	46.1	49.9	52.3	54.4	56.1	57.8	59.1
	Difference	0.0	11.3	17.5	16.5	16.1	13.9	12.4	10.0	7.1	4.6	3.2	2.0	1.5	1.1	1.0
	Cooling	0.0	0.1	0.2	0.4	0.7	1.0	1.0	1.1	1.1	1.1	1.2	1.2	0.9	0.7	0.7
4	Top	10.4	25.2	37.1	41.5	44.9	47.8	50.1	51.7	53.5	54.9	55.7	57	58.1	59.3	60.4
	Bottom	10.4	13.7	19.4	24.3	28.3	33.5	37	41.1	45.5	49.3	51.4	53.8	55.5	57.2	58.6
	Difference	0.0	11.5	17.7	17.2	16.6	14.3	13.1	10.6	8.0	5.6	4.3	3.2	2.6	2.1	1.8
	Cooling	0.0	0.3	0.4	1.1	1.2	1.4	1.7	1.7	2.0	2.1	2.3	2.4	2.0	1.7	1.5
5	Top	10.2	25.1	36.9	41	44.3	47.5	49.9	51.6	53	54.7	55.7	56.6	57.9	59.8	60.6
	Bottom	10.2	13.5	19.3	23.8	27.5	32.4	36	40	44.4	48.3	50.8	53.3	54.9	56.8	58.1
	Difference	0.0	11.6	17.6	17.2	16.8	15.1	13.9	11.6	8.6	6.4	4.9	3.3	3.0	3.0	2.5
	Cooling	0.0	0.4	0.3	1.1	1.4	1.2	1.5	1.7	2.6	2.9	2.9	2.5	2.4	2.6	2.2

Table 8
Temperature test results of SMA-13 mixture.

HGM Dosage (%)	Index	Measured temperature (°C) at different time (h)														
		0.0	0.5	1.0	1.5	2.0	2.5	3.0	3.5	4.0	4.5	5.0	5.5	6.0	6.5	7.0
0	Top	11.9	28.5	39.2	44.7	48.7	51.3	53.8	55.6	57.5	57.9	59.3	60.1	60.6	62.3	63.1
	Bottom	11.9	16.9	22.9	29.1	34.3	38.5	42.2	45.6	48.5	51.0	53.5	55.7	57.6	59.4	60.9
	Difference	0.0	11.6	16.3	15.6	14.4	12.8	11.6	10.0	9.0	6.9	5.8	4.4	3.0	2.9	2.2
3	Top	12.0	28.6	39.4	44.6	48.9	51.5	53.9	55.9	57.8	58.1	59.4	60.3	60.8	62.4	63.3
	Bottom	12.0	17.0	23.0	29.1	34.1	38.2	41.9	45.2	48.1	50.8	53.3	55.6	57.5	59.4	61.0
	Difference	0.0	11.6	16.4	15.5	14.8	13.3	12.0	10.7	9.7	7.3	6.1	4.7	3.3	3.0	2.3
	Cooling	0.0	0.0	0.1	−0.1	0.4	0.5	0.4	0.7	0.7	0.4	0.3	0.3	0.3	0.1	0.1
4	Top	11.7	28.3	39.1	44.6	48.4	51.1	53.5	55.4	57.2	57.8	59.1	59.9	60.4	62.1	62.9
	Bottom	11.7	16.7	22.7	28.7	33.8	37.9	41.5	44.9	47.9	50.5	53.0	55.3	57.2	59.0	60.5
	Difference	0.0	11.6	16.4	15.9	14.6	13.2	12.0	10.5	9.3	7.3	6.1	4.6	3.2	3.1	2.4
	Cooling	0.0	0.0	0.1	0.3	0.2	0.5	0.4	0.5	0.3	0.4	0.3	0.2	0.2	0.2	0.2

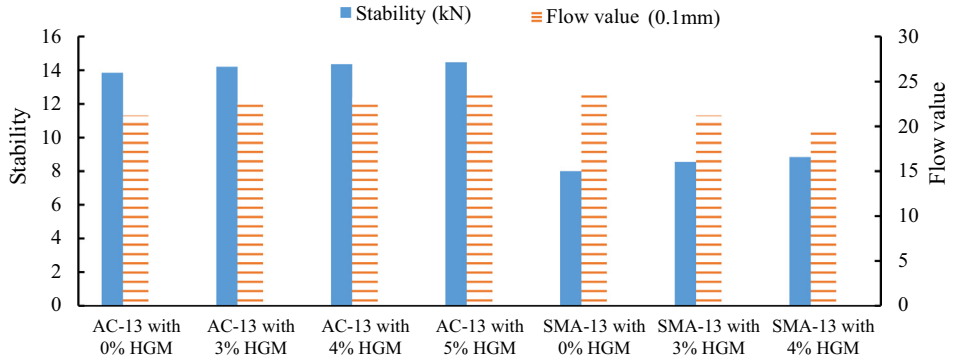

Fig. 7. Marshall test results of asphalt mixtures.

3.3. Pavement performance evaluation

3.3.1. Mechanical property

The Marshall stability and flow value of different asphalt mixtures are shown in Fig. 7. It can be seen that, the addition of HGM increased the flow value of AC-13 mixture to a small extent and almost had no effect on the Marshall stability. For SMA-13, the addition of HGM increased Marshall Stability by a very small extent while decreased flow value.

3.3.2. High temperature stability

Rutting tests were conducted for AC-13 mixture and SMA-13 mixture. The effects of HGM on dynamic stability are shown in Fig. 8. It can be found that the addition of HGM significantly improved the dynamic stability for both AC-13 mixture and SMA-13 mixture, especially for the SMA-13 mixtures. For AC-13 mixture, the addition of 3%, 4% and 5% HGM increased the dynamic stability by 32.9%, 45.9% and 63.6% respectively; for SMA-13 mixture, the addition of 3% and 4% HGM improved the dynamic stability by 50.2% and 83.6%, respectively.

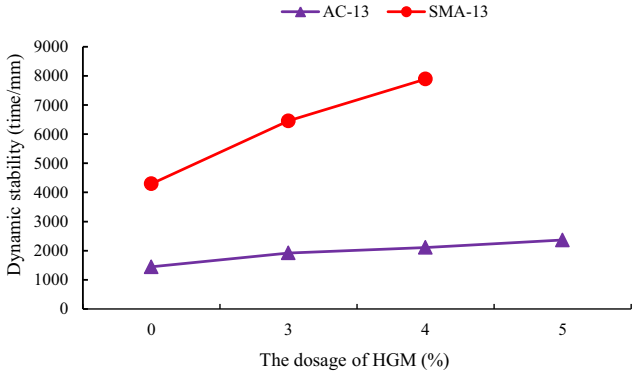

Fig. 8. Wheel tracking test results of asphalt mixture.

This phenomenon can be concluded that the addition of HGM had significant favorable effects on the high temperature stability of asphalt mixture. The increase in the high temperature stability of the asphalt mixture is mainly due to the incorporation of HGM, which increases the content of the asphaltenes, thereby increasing the viscosity of the asphalt. In addition, part of the HGM does not react with the asphalt binder but acts as a small filler to fill the voids of the mixture, which improves the structural properties of the asphalt mixture and increases the adhesion between the aggregate and the asphalt. As a result, the stability of the asphalt mixture at high temperatures was improved [45].

3.3.3. Water stability

For immersion Marshall test, immersion residue stability is the index to characterize the water stability of mixtures, and the results are shown in Fig. 9. It can be seen that, as the amount of HGM increased, the residual stabilities of AC-13 and SMA-13 mixtures both showed a slight increasing trend. The residual stability of AC-13 mixture with 5% HGM increased by 3.5% compared to that of AC-13 without HGM. For SMA-13 mixture, the dosages of 3% and 4% HGM improved the immersion residue stability by 1.9% and 3.3% respectively.

The results of freeze-thaw splitting test is shown in Fig. 10. It can be inferred that, the effects of HGM on *TSR* depend on asphalt mixture type. For AC-13, when 3% or 4% HGM was added, *TSR* almost kept unchanged and then decreased when 5% HGM was added. For SMA-13, the addition of HGM with the content of 3% or 4% decreased the *TSR*. The lowest TSR values for AC-13 and SMA-13 were 83.2% and 80.3%, respectively. According to the specification requirement in China, the *TSR* of AC-13 and SMA-13 need to be greater than or equal to 70 and 80 respectively. Therefore, the lowest *TSR* values can still meet the requirement.

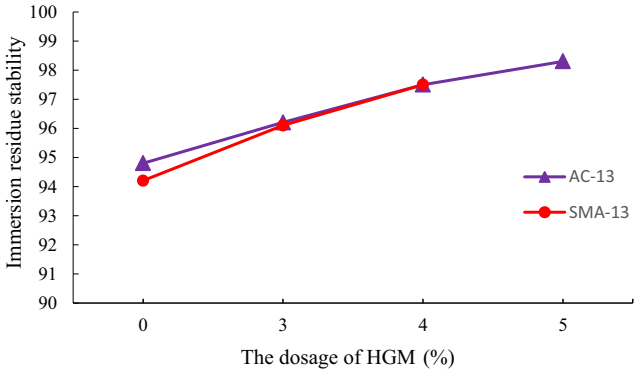

Fig. 9. Immersion Marshall test results of asphalt mixture.

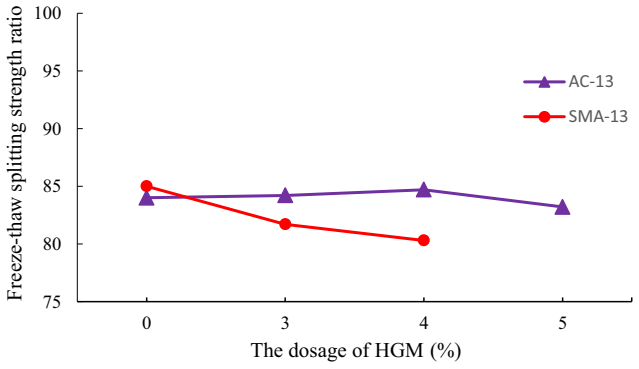

Fig. 10. Freeze-thaw splitting test results of asphalt mixture.

3.3.4. Low temperature crack resistance

The maximum bending strain measured by low temperature bending test was used to evaluate the low temperature crack resistances of AC-13 and SMA-13 mixtures, and the results are shown in Fig. 11. It can be seen that, for AC-13 mixture, with the increase in HGM dosage, the maximum bending strain increased slightly. In contrast, the maximum bending strain of SMA-13 showed a downward trend as the dosage of HGM increased. The additions of 3% and 4% HGM decreased the maximum bending strain by 139.2με and 312.1με respectively. However, the maximum bending strain under 4% HGM was still greater than 2500με which is the specification requirement for SMA in China. It can be concluded that, the addition of HGM improved the low temperature crack resistance of the AC-13 mixture and impaired the low temperature crack resistance of the SMA-13 mixture.

3.3.5. Drainage resistance

For SMA-13 mixture, because of the high asphalt content, Schellenberg binder drainage test was needed to reveal its drainage resistance, and the results are shown in Fig. 12. It can be seen that when 3% HGM was added, the mass loss kept unchanged. While the addition of 4% HGM improved, the mass loss from 0.05% to 0.06%. This means that the addition of HGM may reduce the drainage resistance of SMA-13 mixture. However, the mass loss of the mixture with 4% HGM was still less than 0.1% which is the specification requirement in China.

3.3.6. Scattering resistance

Similar to the drainage resistance, the scattering resistance is only needed by SMA-13 mixture, and the results are shown in Fig. 13. It can be seen that the addition of HGM can reduce the scattering loss and improve the scattering resistance slightly. The scattering resistance of the mixture mainly involved the adhesion between the aggregate and the asphalt. This could be attributed to the fact that part of the HGM in the mixture can absorb the light component into asphaltenes, and another part of the HGM acts as a filler to fill the voids of the mixture, thereby increasing the adhesion between asphalt and aggregate. Therefore, the anti-scattering performance of the mixture was improved.

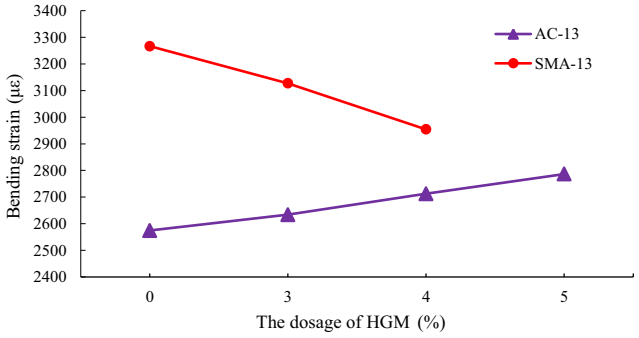

Fig. 11. Low temperature bending test results of asphalt mixtures.

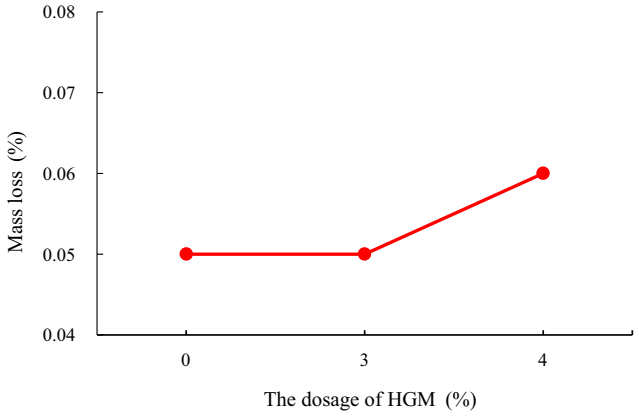

Fig. 12. Schellenberg binder drainage test results of SMA-13 mixture.

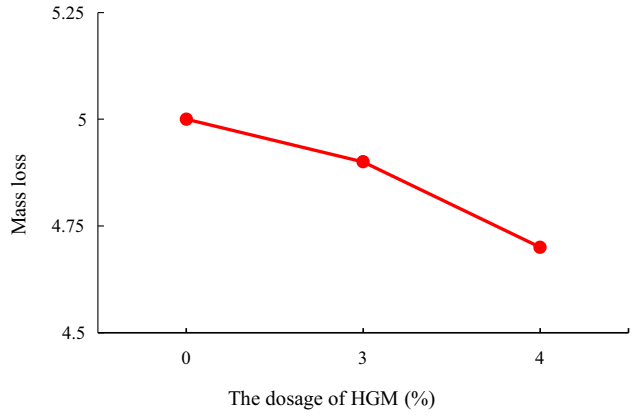

Fig. 13. Cantabro scattering test results of SMA-13 mixture.

3.4. HGM modified asphalt mixture recommendation

As previously discussed in section of cooling performance, the addition of HGM had almost no cooling effect on the SMA-13 mixture, while it had some cooling effects on AC-13 mixture. Therefore, only the optimum content of HGM in AC-13 will be studied.

When the contents of HGM are 3%, 4% and 5% respectively, the cooling effects of the HGM in AC-13 mixture were 1.2 °C, 2.4 °C and

2.9 °C respectively. The cooling effect became better as the content of HGM increased. When the content was 5%, the dynamic stability of AC-13 mixture increased by 63.6% than that of ordinary AC-13 mixtures, the immersion residual stability increased by 3.5%, the freeze-thaw splitting strength ratio decreased by 0.8%, and the low temperature bending strain increased by 8.2%. Therefore, AC-13 with 5% HGM was recommended to be used as the thermal resistance surface layer, and in this case the maximum temperature drop was 2.9 °C.

4. Conclusions

(1) The HGM with the dosages of 3%, 4%, 5% and 6% by weight of asphalt was used to modify matrix and SBS modified asphalt. When it was used to modify matrix asphalt, results showed that with the increase in HGM content, the penetration and ductility decreased, while the softening point increased. When it was used to modify SBS modified asphalt, an increase in the HGM content resulted in a decrease in penetration and ductility while the softening point first increased and then decreased.

(2) The rheological properties of HGM and HGM/SBS modified asphalts were tested and the results showed that with the increase in the amount of HGM, the high temperature shear resistance of asphalt increased while the low temperature crack resistance decreased.

(3) A temperature system was designed and used to test the cooling performance of AC-13 and SMA-13 mixtures with different contents of HGM. The addition of HGM improved the cooling performance of AC-13 while it had no obvious influence on the cooling performance of SMA-13.

(4) The addition of HGM had some different influences on the performances of asphalt mixture. For AC-13 mixture, it improved the Marshall stability, high-temperature stability, low-temperature cracking resistance and immersion residue stability while exhibiting insignificant on *TSR*. For SMA-13 mixture, it improved the Marshall stability, high-temperature stability, immersion residue stability, scattering resistance while decreasing the low-temperature crack resistance, *TSR* and anti-drainage ability.

(5) According to the cooling effect and road performance, it was recommended to use 5% HGM modified AC-13 mixture as the thermal resistance surface layer, and in this case the maximum temperature drop was about 2.9 °C.

Declaration of Competing Interest

None declared.

Acknowledgement

This research was supported by the Natural Science Basic Research Plan in Guangdong Provincial Communication Department (No. 2016 - 611) and the Key Science and Technology Project in Dongying City (No. 2016 - 20) and Fundamental Research Funds for the Central Universities of Chang'an University (300102218523). This support is gratefully acknowledged.

References

[1] G. Wang, R. Roque, D. Morian, Effects of surface rutting on near-surface pavement responses based on a two-dimensional axle-tire-pavement interaction finite-element model, J. Mater. Civ. Eng. 24 (11) (2012) 1388–1395, https://doi.org/10.1061/(ASCE)MT.1943-5533.0000526.

[2] J.T. Kevern, L. Haselbach, V.R. Schaefer, Hot weather comparative heat balances in pervious concrete and impervious concrete pavement systems, J. Heat Isl. Inst. Int. 7 (2) (2012) 231–237, https://doi.org/10.1016/j.enbuild.2014.09.076.

[3] K.A. Gray, M.E. Finster, The Urban Heat Island, Photochemical Smog and Chicago: Local Features of the Problem and Solution, Northwestern University Department of Civil Engineering, 1999.

[4] M. Santamouris, N. Gaitani, A. Spanou, M. Saliari, K. Giannopoulou, K. Vasilakopoulou, T. Kardomateas, Using cool paving materials to improve microclimate of urban areas-design realization and results of the flisvos project, Build. Environ. 53 (7) (2012) 128–136, https://doi.org/10.1016/j.buildenv.2012.01.022.

[5] Y.F. Du, Q. Shi, S.Y. Wang, Highly oriented heat-induced structure of asphalt pavement for reducing pavement temperature, Energy Build. 85 (12) (2014) 23–31, https://doi.org/10.1016/j.enbuild.2014.09.035.

[6] A.M. Sha, Z.Z. Liu, K. Tang, P.Y. Li, Solar heating reflective coating layer (SHRCL) to cool the asphalt pavement surface, Constr. Build. Mater. 139 (5) (2017) 355–364, https://doi.org/10.1016/j.conbuildmat.2017.02.087.

[7] T. Inoue, T. Shimo, M. Ichinose, K. Takase, T. Nagahama, Improvement of urban thermal environment by wavelength-selective retro-reflective film, Energy Procedia 122 (9) (2017) 967–972, https://doi.org/10.1016/j.egypro.2017.07.447.

[8] Y.L. Cheng, X.Q. Zhang, C.Q. Fang, J. Chen, Z, Wang, Discoloration mechanism, structures and recent applications of thermochromic materials via different methods: a review, J. Mater. Sci. Technol. 34 (12) (2018) 2225–2234, https://doi.org/10.1016/j.jmst.2018.05.016.

[9] S.J. Zheng, Y. Xu, Q.H. Shen, H. Yang, Preparation of thermochromic coatings and their energy saving analysis, Sol. Energy 112 (2) (2015) 263–271, https://doi.org/10.1016/j.solener.2014.09.049.

[10] Z. Refaa, M.R. Kakar, A. Stamatiou, J. Worlitschek, M.N. Partl, M. Bueno, Numerical study on the effect of phase change materials on heat transfer in asphalt concrete, Int. J. Therm. Sci. 133 (11) (2018) 140–150, https://doi.org/10.1016/j.ijthermalsci.2018.07.014.

[11] D. Zhang, M.Z. Chen, S.P. Wu, Q.T. Liu, J.M. Wan, Preparation of expanded graphite/polyethylene glycol composite phase change material for thermoregulation of asphalt binder, Constr. Build. Mater. 169 (4) (2018) 513–521, https://doi.org/10.1016/j.conbuildmat.2018.02.167.

[12] B. Athukorallage, T. Dissanayaka, S. Senadheera, D. James, Performance analysis of incorporating phase change materials in asphalt concrete pavements, Constr. Build. Mater. 164 (3) (2018) 419–432, https://doi.org/10.1016/j.conbuildmat.2017.12.226.

[13] G. Guldentops, A.M. Nejad, C. Vuye, W.V.D. Bergh, N. Rahbar, Performance of a pavement solar energy collector: Model development and validation, Appl. Energy 163 (2) (2016) 180–189, https://doi.org/10.1016/j.apenergy.2015.11.010.

[14] D.S.N.M. Nasir, B.R. Hughes, J.K. Calautit, A CFD analysis of several design parameters of a road pavement solar collector (RPSC) for urban application, Appl. Energy 186 (1) (2017) 436–449, https://doi.org/10.1016/j.apenergy.2016.04.002.

[15] T.H. Cahill, M. Adams, C. Marm, Storm water management with porous pavements, Government Engineering (2005) 14–19.

[16] Y. Liu, T. Li, H.Y. Peng, A new structure of permeable pavement for mitigating urban heat island, Sci. Total Environ. 634 (9) (2018) 1119–1125, https://doi.org/10.1016/j.scitotenv.2018.04.041.

[17] J. Chen, X.J. Yin, H. Wang, Y.M. Ding, Evaluation of durability and functional performance of porous polyurethane mixture in porous pavement, J. Cleaner Prod. 188 (7) (2018) 12–19, https://doi.org/10.1016/j.jclepro.2018.03.297.

[18] H. Higashiyamaa, M. Sanob, F. Nakanishic, O. Takahashid, S. Tsukumad, Field measurements of road surface temperature of several asphalt pavements with temperature rise reducing function, Case Stud. Constr. Mater. 4 (6) (2016) 73–80, https://doi.org/10.1016/j.cscm.2016.01.001.

[19] J. Wanga, Q. Menga, K. Tana, L. Zhanga, Y. Zhang, Experimental investigation on the influence of evaporative cooling of permeable pavements on outdoor thermal environment, Build. Environ. 140 (8) (2018) 184–193, https://doi.org/10.1016/j.buildenv.2018.05.033.

[20] R.S. Benrazavi, K.B. Dolaa, N. Ujanga, N.S. Benrazavi, Effect of pavement materials on surface temperatures in tropical environment, Sustainable Cities Soc. 22 (4) (2016) 94–103, https://doi.org/10.1016/j.scs.2016.01.011.

[21] M.Z. Chen, J. Zheng, F.Z. Li, S.P. Wu, J.T. Lin, L. Wan, Thermal performances of asphalt mixtures using recycled tyre rubber as mineral filler, Road Mater. Pavement Des. 16 (1) (2015) 379–391, https://doi.org/10.1080/14680629.2014.1002524.

[22] J. Liu, Research on Thermal Resistance Pavement Materials, Chang'an University, 2009.

[23] F.L. Yang, Study on Application of Vermiculite in the Thermal Resistance Pavement, Chang'an University, 2012.

[24] Q.H. Zhao, Experimental study on ceramsite thermal resistance wear layer materials, Chang'an University, 2012.

[25] S.N. Patankar, Y.A. Kranov, Hollow glass microsphere HDPE composites for low energy sustainability, Mater. Sci. Eng.: A 527 (3) (2010) 1361–1366, https://doi.org/10.1016/j.msea.2009.10.019.

[26] K. Ahn, M. Kim, K. Kim, H. Ju, I. Oh, J. Kim, Fabrication of low-methanol permeability sulfonated poly (phenylene oxide) membranes with hollow glass microspheres for direct methanol fuel cells, J. Power Sour. 276 (2) (2015) 309–319, https://doi.org/10.1016/j.jpowsour.2014.11.114.

[27] B.L. Zhu, J. Wang, H. Zheng, J. Ma, J. Wu, R. Wu, Investigation of thermal conductivity and dielectric properties of LDPE-matrix composites filled with

hybrid filler of hollow glass microspheres and nitride particles, Compos. B 69 (2) (2015) 496–506, https://doi.org/10.1016/j.compositesb.2014.10.035.
[28] M.M. Ashton-Patton, M.M. Hall, J.E. Shelby, Formation of low density polyethylene/hollow glass microspheres composites, J. Non-Cryst. Solids 352 (5) (2006) 615–619, https://doi.org/10.1016/j.jnoncrysol.2005.11.058.
[29] L.A. Dombrovsky, J.H. Randrianalisoa, D. Baillis, Infrared radiative properties of polymer coatings containing hollow microspheres, Int. J. Heat Mass Transf. 50 (4) (2007) 1516–1527, https://doi.org/10.1016/j.ijheatmasstransfer.2006.08.034.
[30] S.C. Kim, D.K. Lee, Preparation of TiO2-coated hollow glass beads and their application to the control of algal growth in eutrophic water, Microchem. J. 80 (6) (2005) 227–232, https://doi.org/10.1016/j.microc.2004.07.008.
[31] L. Sun, S. Wan, Z. Yu, L. Wang, Optimization and modeling of preparation conditions of TiO2 nanoparticles coated on hollow glass microspheres using response surface methodology, Sep. Purif. Technol. 125 (4) (2014) 156–162, https://doi.org/10.1016/j.seppur.2014.01.042.
[32] D.H. Lu, Q. Gao, X.M. Wu, Y.M. Fan, ZnO nanostructures decorated hollow glass microspheres as near infrared reflective pigment, Ceram. Int. 43 (8) (2017) 9164–9170, https://doi.org/10.1016/j.ceramint.2017.04.067.
[33] M.Y. Han, Study on thermodynamic properties of hollow glass microbeads cement-based composites, Henan University of Technology, 2014.
[34] The Industry Standards of the People's Republic of China, JTG E20-2011, Standard Test Methods of Bitumen and Bituminous Mixture for Highway Engineering, China Communications Press, Beijing, 2011.
[35] The Industry Standards of the People's Republic of China, JTG F40-2004, Technical Specification for Construction of Highway Asphalt Pavement, China Communications Press, Beijing, 2004.
[36] ASTM D6927-15, Standard Test Method for Marshall Stability and Flow of Asphalt Mixtures, ASTM International, West Conshohocken, PA, 2015, https://doi.org/10.1520/D6927-15
[37] ASTM D5 / D5M-13, Standard Test Method for Penetration of Bituminous Materials, ASTM International, West Conshohocken, PA, 2013. https://doi.org/10.1520/D0005_D0005M-13
[38] ASTM D36 / D36M-14e1, Standard Test Method for Softening Point of Bitumen (Ring-and-Ball Apparatus), ASTM International, West Conshohocken, PA, 2014. https://doi.org/10.1520/D0036_D0036M-14E013
[39] ASTM D113-17, Standard Test Method for Ductility of Asphalt Materials, ASTM International, West Conshohocken, PA, 2017. https://doi.org/10.1520/D0113-17
[40] ASTM D7175-15, Standard Test Method for Determining the Rheological Properties of Asphalt Binder Using a Dynamic Shear Rheometer, ASTM International, West Conshohocken, PA, 2015 https://doi.org/10.1520/D7175-15
[41] ASTM D6648-08(2016), Standard Test Method for Determining the Flexural Creep Stiffness of Asphalt Binder Using the Bending Beam Rheometer (BBR), ASTM International, West Conshohocken, PA, 2016 https://doi.org/10.1520/D6648-08R16
[42] AASHTO, AASHTO T 283, Standard Method of Test for Resistance of Compacted Asphalt Mixture to Moisture-Induced Damage, AASHTO, 2003.
[43] F. Ma, C. Zhang, Z. Fu, Study on road performance and mechanism of nano calcium carbonate modified asphalt, J. Wuhan Univ. Technol. (Transp. Sci. Eng.) 31 (2) (2007) 88–91.
[44] F. Ma, Study on road performance and modification mechanism of nanometer calcium carbonate modified asphalt, Chang'an University, 2004.
[45] L.C. Cai, X.A. Shi, J. Xue, Laboratory evaluation of composed modified asphalt binder and mixture containing nano-silica/rock asphalt/SBS, Constr. Build. Mater. 172 (5) (2018) 204–211, https://doi.org/10.1016/j.conbuildmat.2018.03.187.